

This is a preprint of an article published in

Advances in Civil Engineering materials (ACEM) – Volume 2, #1, 2013

ISSN: 2165-3984;

CODEN: ACEMF9

Paper ID: ACEM104469

DOI: 10.1520/ACEM104469

The final and published paper can be found at

http://www.astm.org/DIGITAL_LIBRARY/JOURNALS/ACEM/PAGES/ACEM20120003.htm

Development of a Reference Material for the Calibration of Cement Paste Rheometers

REFERENCE: Ferraris, Chiara F., Li, Zhuguo, Zhang, Min-Hong, and Stutzman, Paul, "Development of a Reference Material for the Calibration of Cement Paste Rheometers," *Advances in Civil Engineering Materials*, Vol. 2, No. 1, 2013, pp. 140–162, doi:10.1520/ACEM20120003. ISSN 2165-3984.

ABSTRACT: Rheometers for measuring the properties of fluids are usually calibrated using a standard reference oil. However, a rheometer used for concrete cannot be calibrated using an oil, because of the unusual geometry and size. It would be advantageous to have a granular reference material. A material that can simulate a Bingham fluid, such as cement paste, was developed in this study as a mixture of corn syrup, water, and fine limestone. This reference material will form the basis of future mortar and concrete reference materials containing fine and coarse aggregates. This paper illustrates the various aspects of the development and shows data obtained using various geometries of rheometers.

KEYWORDS: cement paste, rheometer, reference material, Bingham rheological parameters

Nomenclature

h = gap or distance between the plates, mm

L = length of the bob, m

n = speed of rotation of the top plate, revolutions (1/s)

R_b = diameter of the bob, m

R_p = radius of shear, mm (17.5 mm in our case)

T = torque, N · m

T_e = torque at the outer edge, N · m

$\dot{\gamma}$ = shear rate

$\dot{\gamma}_R$ = shear rate at the outer edge (1/s)

μ_{pl} = plastic viscosity

τ = shear stress, Pa

τ_B = Bingham yield stress

Introduction

Rheological measurements are often performed using a rotational rheometer. In this type of rheometer, the tested fluid is sheared between two surfaces, one of which is rotating [1]. The rate of the rotating surface is usually precisely controlled with a computer, and the torque resulting from

Manuscript received February 10, 2012; accepted for publication March 5, 2013; published online April 17, 2013.

¹Materials & Structures Systems Division, Engineering Laboratory, National Institute of Standards and Technology (NIST), 100 Bureau Dr., MS 8615, Gaithersburg, MD 20899, USA (Corresponding author), e-mail: clarissa@nist.gov

²Graduate School of Science and Engineering, Yamaguchi Univ., 2-16-1, Tokiwadai, Ube, Yamaguchi, 755-8611, Japan, e-mail: li@yamaguchi-u.ac.jp

³Dept. of Civil Engineering, National Univ. of Singapore, 1 Engineering Dr. 2, Singapore 117576, Singapore, e-mail: mhzhang@nus.edu.sg

⁴Materials & Structures Systems Division, Engineering Laboratory, National Institute of Standards and Technology (NIST), 100 Bureau Dr., MS 8615, Gaithersburg, MD 20899, United States of America, e-mail: paul.stutzman@nist.gov

the material response is measured. Laboratory rheometers are mainly designed for homogeneous liquids containing no particles, such as oils. The manufacturers recommend using a standard oil of known viscosity to verify that the instrument is operating correctly. The kinematic viscosities of fluids are determined through reference to the water viscosity established by international consensus in 1953 [2], as described in ISO-3666 [3]. In 1954, the National Institute of Standards and Technology (NIST) [2] conducted a study to compare two instruments, the Bingham viscometer and the Cannon Master viscometer (both based on capillary flow), that are still used for determining the viscosity values of standard oils.

Because these standard oils are expensive, however, they cannot be used for the large volumes employed in concrete rheometers. Some concrete rheometers have used a less expensive oil with a known viscosity, as measured using a calibrated rheometer. In 2003, a high viscosity polydimethylsiloxane fluid (with a NIST-measured viscosity of $29.5 \text{ Pa} \cdot \text{s} \pm 0.6 \text{ Pa} \cdot \text{s}$ at $24.4^\circ\text{C} \pm 0.4^\circ\text{C}$) was used in concrete rheometers [4] during an international round-robin. It was shown that not all rheometers were able to measure the oil properties because of their specific shear patterns and slippage on the shearing surfaces. In the case of fresh concrete, the geometry of the rheometer needs to allow the distance between the shearing surfaces to be sufficiently large to accommodate aggregates at least 5 mm in diameter. The increase in the gap size leads to generally unknown shear patterns and test results that cannot be expressed in fundamental units. Therefore, it is almost impossible to calibrate such large and non-standard rheometers using the traditional method involving oils, because of the lack of an analytical solution for the shear stress fields between the two shearing surfaces. Nevertheless, any two concrete rheometers were found to be correlated, and all rheometers ranked the concrete tested in the same order in terms of viscosity and yield stress [5,6].

Ferraris et al. [7] calibrated various rotational rheometer geometries using standard oil and successfully determined a correction factor for a small rheometer geometry used for mortar. A reference material is needed for the calibration of rheometers with complex geometries. A relatively inexpensive, safe reference material is needed that incorporates aggregates for concrete rheometers. As concrete and mortars are non-Newtonian, the reference material also should be non-Newtonian.

One solution would be to develop a granular reference material, similar to concrete, of known rheological properties. ACI Committee 238 on Workability of Fresh Concrete discussed this issue, and one of their first ideas was to use an oil of known viscosity and then add particles. The particles should be spherical to simplify the simulation of the increased viscosity due to an increase in solid concentration. Moreover, the particle specific gravity should match that of the oil so as to avoid sedimentation during testing. According to these conditions, hollow plastic spheres would be suitable. Unfortunately, their cost is prohibitive (over \$3000 per batch of 20 L). Therefore, the idea was abandoned, and it was determined that a multiphase approach would be better. Other authors have investigated granular materials as ideal materials for rheological properties or calibration, such as carbopol [8] and calcium carbonate [9]. In both cases the pH needs to be adjusted. This paper explores other solutions for the development of a reference material that would not require pH adjustment, thus simplifying the mixture.

The multiphase approach consists of developing a paste that can be measured with a conventional rheometer. A mortar is produced by adding sand to the paste, and finally a concrete is formed through the addition of coarse aggregates. The rheological parameters of mortar and concrete would be determined from the paste via a combination of numerical simulations and experimental measurements. The simulation should be able to calculate the viscosity of the suspensions

(mortar or concrete) from the medium viscosity (cement paste) with various aggregate concentrations, aggregate size distribution, and particle shape. However, a reference material to represent cement paste does not exist at this time and needs to be developed. This approach will be used to develop a series of three reference materials: paste (presented in this paper), mortar (this reference material with fine beads), and concrete (mortar with coarser beads). The last two reference materials will be developed in future years.

A non-Newtonian reference material for cement paste should have the following characteristics: (1) no particle segregation for the duration of the test; (2) a linear Bingham stress response to shear rates over a large range (e.g., 1 s^{-1} to 50 s^{-1} [10]); (3) rheological and chemical properties that remain unchanged over a long period of time (i.e., days or weeks) with no chemical reactions between the medium and the particles; (4) a yield stress sufficient to avoid the segregation of added fine and coarse aggregates, so that it can be used to produce a reference material for mortar and concrete (e.g., Saak et al. [11] suggested a yield stress of over 60 Pa for cement paste); and (5) a reversible linear response, implying no structural breakdown or build-up, flocculation, or deflocculation during the test (i.e., no hysteresis in the flow curve [increasing and decreasing shear rate]).

This paper explores some potential reference material candidates for a paste with the required characteristics (replacement of the cement paste). A proposed reference material will be further tested via determination of its rheological properties using several geometries. Some shelf life studies also are presented. Investigations on mortar and concrete, including simulations, will be presented in future papers.

Background

Rheological measurements typically produce a shear stress–shear rate plot. In cases when the geometry of the rheometer does not allow a direct calculation of the shear stress and shear rate in fundamental units, the rotational speeds and the resulting torques are plotted [10].

The viscosity [1] is defined as the ratio of the shear stress to the shear rate at a given shear rate. For a Newtonian fluid, it is also equal to the slope of the fitted line of the shear stress–shear rate plot, going through zero, as the relationship is linear. But most granular materials are non-Newtonian. Their main characteristic is that they exhibit a yield stress, which is the stress needed to initiate deformation or flow of the material. There are several methods for measuring the yield stress. The two most common methods are the stress growth method and extrapolation from the Bingham test method [12,13]. In the case of the stress growth method, a small shear rate is applied and the induced shear stress is monitored. This stress increases linearly until the sample yields and starts to flow. Figure 1 shows the various stages of this test.

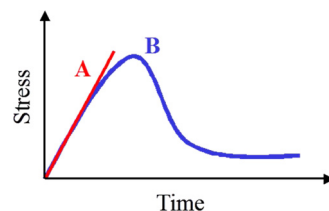


FIG. 1—Stress growth schematic. Point A is the end of the linear portion (i.e., elastic limit), and it is considered as the static yield stress point. Point B is the peak stress associated with the dynamic yield stress, and it is taken as an approximation of the true yield stress because it is easier to determine than point A.

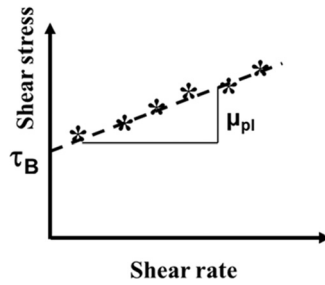


FIG. 2—Bingham model and calculation of the plastic viscosity and yield stress.

Most researchers use the method based on the Bingham equation (Eq 1) to determine the plastic viscosity and the yield stress. This procedure implies that the plastic viscosity is defined as the slope of the shear stress–shear rate curve and the yield stress is the intercept of the curve at zero shear rate. This point is generally not measured, so this constitutes an extrapolation (Fig. 2). The Bingham rheological parameters, yield stress, and plastic viscosity characterize the flow curve within a range of shear rates, as shown in Fig. 2 and Eq 1.

$$\tau = \tau_B + \mu_{pl}\dot{\gamma} \tag{1}$$

where:

- τ = shear stress,
- τ_B = Bingham yield stress,
- μ_{pl} = plastic viscosity, and
- $\dot{\gamma}$ = shear rate.

Some preliminary work was done to identify a suitable reference material that fulfilled all the requirements described in the Introduction. Some candidates examined were fly ash–oil suspensions and slag–water–high range water reducer admixture (HRWRA) combinations [14]. Some reasonable results were obtained, but these materials did not fulfill all the requirements. For instance, the slag–water mixture had a tendency to segregate, and the fly ash–oil suspension was expensive because of the cost of the oil.

In this paper, we describe the development of a suitable material that corresponds to the criteria mentioned above. The rheological parameters in Eq 1 are calculated using the Bingham equation.

Materials Tested

The materials tested were fine particles in a Newtonian medium (Table 1). The viscosity of the each medium was also measured.

TABLE 1—Summary of materials used.

Particle Type	Medium
Silica fume or quartz	Water
Welan gum	Water
Limestone	Corn syrup and water solution

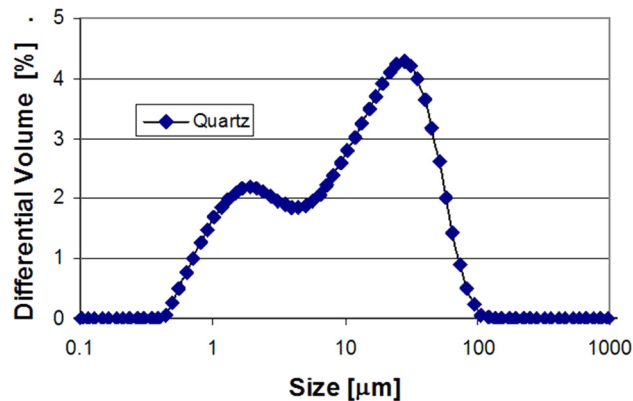


FIG. 3—Particle size distributions of the quartz and the silica fume measured via laser diffraction in isopropanol.

Silica Fume and Quartz in Water

The silica fume (SF) had a density of $2550 \text{ kg/m}^3 \pm 10 \text{ kg/m}^3$. The composition, as provided by the manufacturer, was 93 % silica (SiO_2) and less than 0.7 % each of the following compounds: Al_2O_3 , Fe_2O_3 , MgO , CaO , Na_2O , and K_2O . Loss on ignition (LOI) was less than 6 %.

The quartz powder had a density of $2670 \text{ kg/m}^3 \pm 10 \text{ kg/m}^3$. The particle size distribution (PSD) is shown in Fig. 3. The quartz PSD was bimodal.

Welan Gum

Welan gum suspension was prepared by mixing welan gum powder in water with a high shear blender. The concentration of the welan gum was 3.5 % by mass. The water pH was adjusted to 11. A biocide was also added to prevent this natural product from degrading rapidly (degradation typically took place within a few days).

Corn Syrup and Limestone Powder

Two types of corn syrup and three types of limestone were used. Two corn syrups were obtained from two sources and were characterized for water content and sugar composition. The water content was determined using a volumetric Karl Fischer Titration with a 50/50 mixture of methanol/formamide as the solvent. The chemical composition of the sugar was determined via ion chromatography.

- Corn syrup 1 (CS-US) was, according to the manufacturer, pure corn syrup with no additives. Its density measured at NIST was $1427 \text{ kg/m}^3 \pm 5 \text{ kg/m}^3$, its water content was $18.6\% \pm 0.2\%$ by mass, and the chemical composition was 100 % glucose.
- Corn syrup 2 (CS-J) was, according to the manufacturer, a 75.4 % aqueous solution of pure corn syrup with pH 4.48. Its density as measured at NIST was $1387 \text{ kg/m}^3 \pm 5 \text{ kg/m}^3$. The water content as measured at NIST was $24\% \pm 0.2\%$ by mass fraction, similar to the amount declared by the manufacturer. The chemical composition was 43 % glucose and 57 % fructose by mass fraction.

Three limestone powders were obtained from two sources in the United States and Japan.

- L-US (United States) is also referred to by the manufacturer as micro-limestone flour.
- L-J (Japan) is also referred to by the manufacturer as limestone flour.
- L-JFine (Japan) is sold by the manufacturer as a powder composed of smaller particles than L-J.

TABLE 2—Properties of the limestone used.

	Material		
	L-US	L-J	L-Jfine
Density, kg/m ³	2755 ± 5	2750 ± 5	2800 ± 5
BET surface, m ² /g	1.56 ± 0.04	1.17 ± 0.02	1.78 ± 0.02
Phases, %			
Calcite	75 ± 2.6	94.1 ± 0.1	96.6 ± 0.7
Dolomite	20 ± 2.1	4.7 ± 0.1	1.4 ± 0.1
Quartz	0.8 ± 0.7	0.4 ± 0.1	0.2 ± 0.1
Tremolite	2 ± 0.8		
Talc	0.8 ± 0.2		
Chlorite	0.7 ± 0.7	0.4 ± 0.1	0.5 ± 0.1

The limestone powders were analyzed to determine mineralogical, chemical, and physical differences. Table 2 and Fig. 4 show some physical properties and the PSDs, respectively.

The PSD was measured using either water or isopropanol as the suspension media. It should be noted that there is little difference, and the particles are assumed to be well dispersed in either medium. The difference of the maximum particle size between L-J and L-US is due to the difference in production. The L-US is sieved with a #325 sieve (45 μm opening), whereas the L-J is sieved with a #100 sieve (150 μm opening).

Based on the results in Table 2 and Fig. 4, the main differences among the limestone from the United States and the two from Japan are the following:

- The L-J has a bi-modal distribution of particle sizes.
- The L-US and L-JFine both have a narrow distribution, but clearly L-JFine is finer than L-US. The surface area of L-JFine is 14 % larger than that of L-US. This is further shown by the difference in the median particle sizes (d_{50}), which were 5 μm for L-JFine and 15 μm for L-US.

These differences would play a major role in determining the rheological properties, especially the degree to which the fine particles increase viscosity and yield stress [13–15]. An explanation for this is that the greater concentration of fine particles increases the number of contacts between the particles, creating more friction.

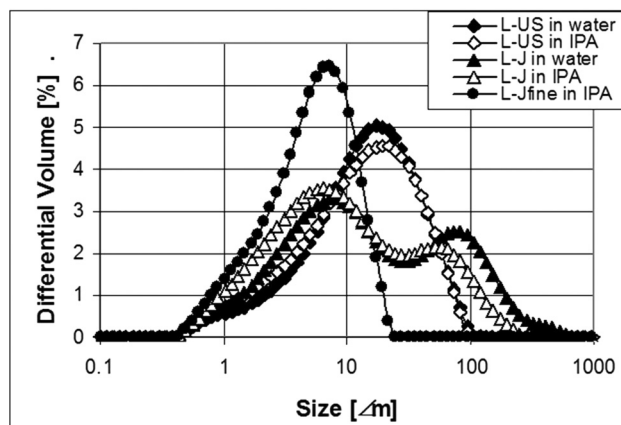


FIG. 4—Particle size distribution of the limestone particles measured via laser diffraction in isopropanol and in water.

Mineralogical analysis via x-ray powder diffraction is based upon replicate bulk analyses, and the analysis of a 10 % hydrochloric acid extraction of the carbonate phases to concentrate the insoluble residue was performed on the three limestones. The insoluble residue is typically composed of quartz, clays, and other minerals unaffected by the dissolution process. The residue is pipetted onto a glass slide to facilitate identification of the clay minerals, and the slide is analyzed after three treatments: heating to 110°C to collapse any expandable clays, saturation in a 50 % ethylene glycol solution to expand the basal spacing of any expandable clays, and heating to 550°C to collapse the layers completely and decompose specific clay minerals. The most reliable numbers are those of the carbonates and quartz. Insoluble residues amounted to about 2.5 % for L-US and about 1 % for L-J and L-JFine. These were a bit difficult to assess, as the mass of the residue was so small. The residue also appeared deliquescent, confounding the insoluble residue analysis.

L-US differed in that it had substantially more dolomite, as well as a slightly greater amount of insoluble residue. This residue comprised tremolite, quartz, talc, a chlorite/smectite inter-stratified clay, and an illite/mica. The presence of talc and tremolite is not uncommon in limestones exposed to some metamorphic processes. Scanning electron microscopy (SEM) pictures at various magnifications are shown in Fig. 5.

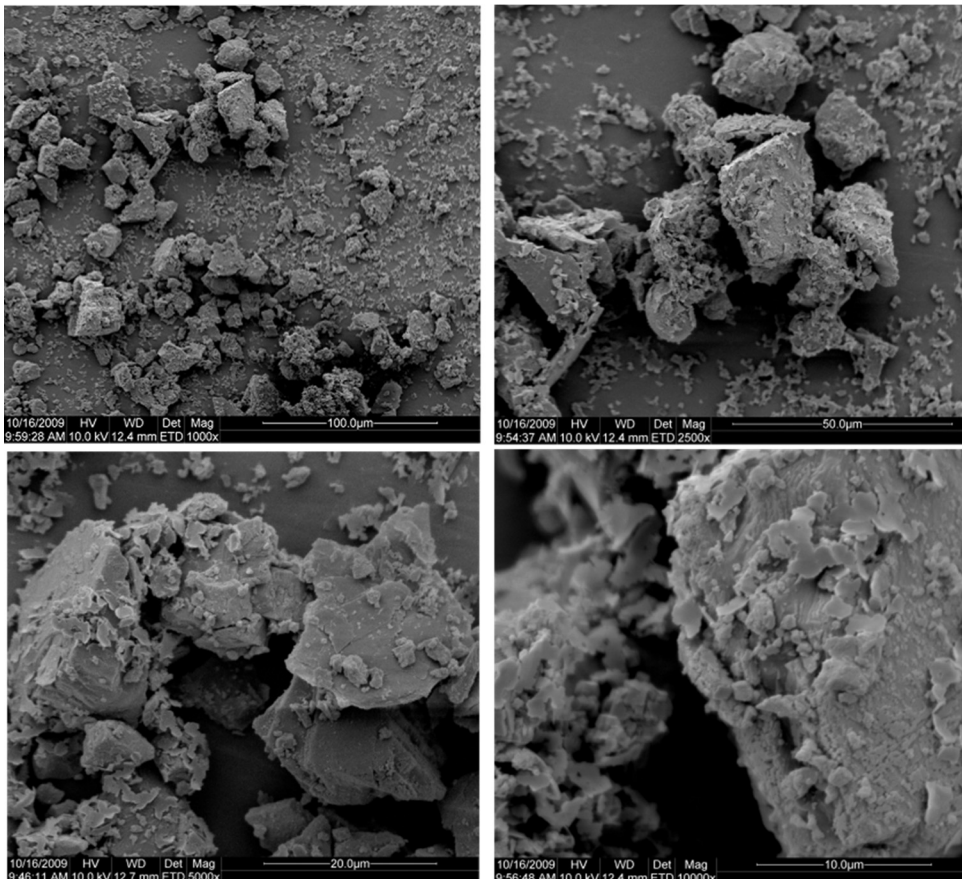


FIG. 5—L-US SEM pictures at various magnifications as indicated by scale bars in the pictures.

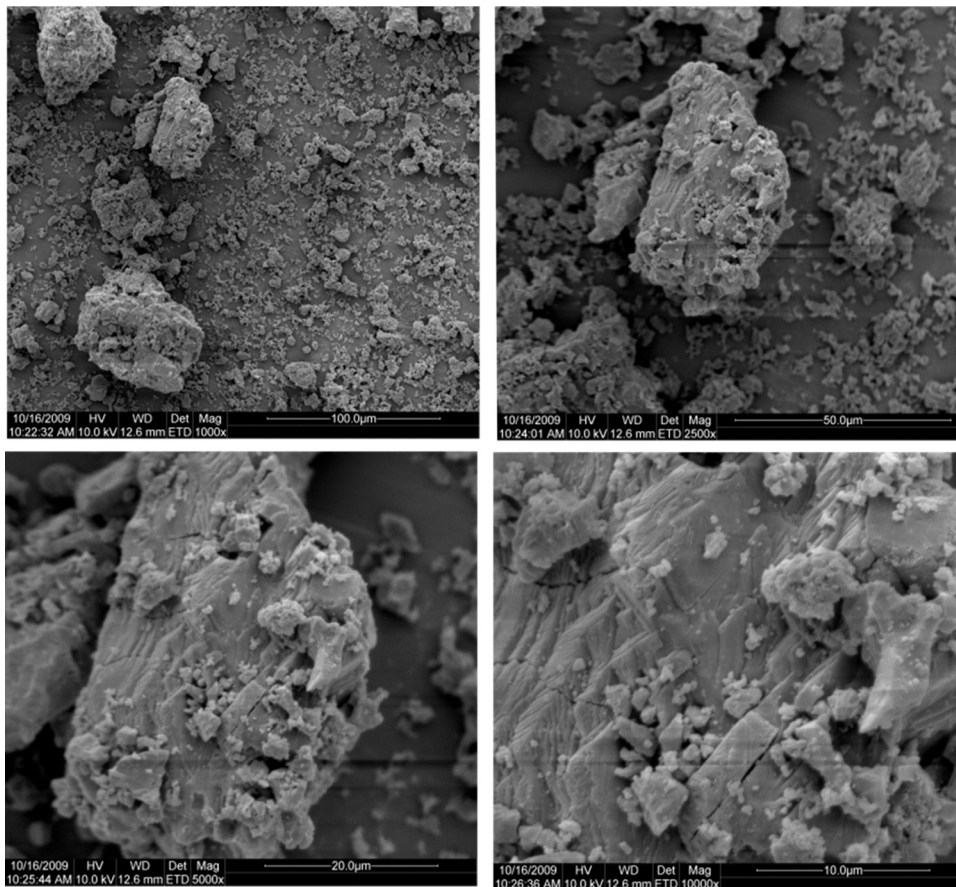


FIG. 6—L-J SEM pictures at various magnifications as indicated by scale bars in the pictures.

L-J and L-JFine had greater amounts of calcite and less insoluble residue, which comprised primarily quartz and chlorite. L-J and L-JFine differ from each other in the content of dolomite, and L-JFine might have slightly more insoluble residue. SEM pictures at various magnifications are shown in Figs. 6 and 7 for L-J and L-JFine, respectively. The SEM images are given to show the morphological differences among the various limestones.

Experimental Setup

All preliminary tests were performed using a rotational rheometer equipped with a parallel plate geometry. The plates were 35 mm in diameter and were serrated [7,14,16] to avoid slippage [17,18]. The gap between the two plates was 0.4 mm for the development phase of the program. Then, other gaps were used to determine the effect of the gap on the results.

To homogenize the material prior to the measurement of the rheological parameters via the Bingham method, a shear rate of 0.1 s^{-1} was applied first for 200 s, and after a rest of 30 s the shear rate was increased from 0.1 s^{-1} to 50 s^{-1} and then decreased back to 0.1 s^{-1} . The induced shear stresses were measured, corresponding to 15 levels of shear rates on the up curve and 20 levels on the down curve. Each measured point was recorded after the shear stress reached equilibrium or after 30 s, whichever occurred first. The descending data were linearly fit (Fig. 2), and the slope and intercept

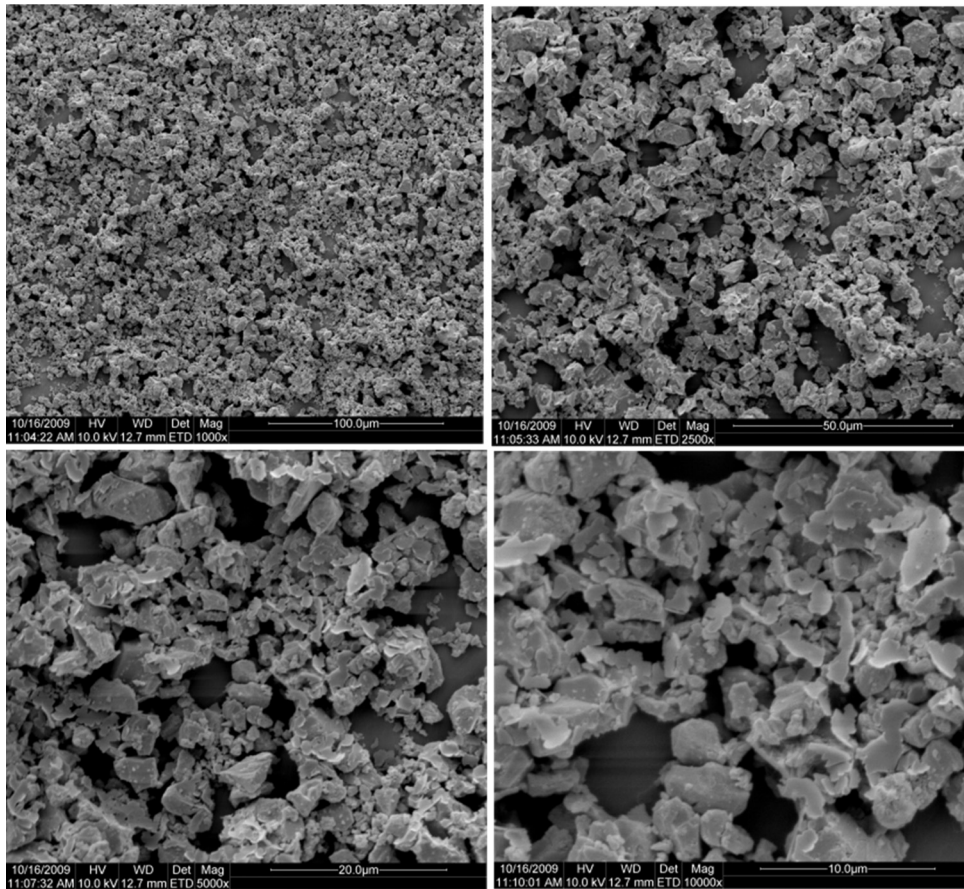


FIG. 7—*L-J Fine SEM pictures at various magnifications as indicated by scale bars in the pictures.*

were calculated. This maximum shear rate value was selected to be high enough to match that in concrete placement [19]. Saak et al. [11] state that the shear rate during placement is about 40 s^{-1} .

Two other geometries, coaxial and vane, were used to verify that the material developed was suitable for other rheometers as well. The coaxial rheometers had the following two different dimensions:

- Coaxial A: a gap of 2.5 mm, a cup diameter of 43 mm, and a bob diameter of 38 mm. The length of the bob was 55 mm (Fig. 8). The coaxial A bob was made of stainless steel, and the surfaces were smooth.
- Coaxial B [20]: a gap of 4.9 mm, a cup diameter of 43 mm, and an overall bob diameter of 33.2 mm. The length of the bob was 69.4 mm (Fig. 8). The bob was made of plastic covered with waterproof sand paper grit 100 for the serrated version and covered in electrical tape for the smooth-surface version. The diameter of the bob was measured with the covers.

The coaxial B bob was fabricated at NIST [20], and the coaxial A bob was purchased with the rheometer. The same container was used for both bobs (diameter = 43 mm).

The vane geometry had the following dimensions: container of 43 mm (same as used for the coaxial), vane diameter of 22 mm, and vane length of 16 mm. The vane was a simple cross with four blades.

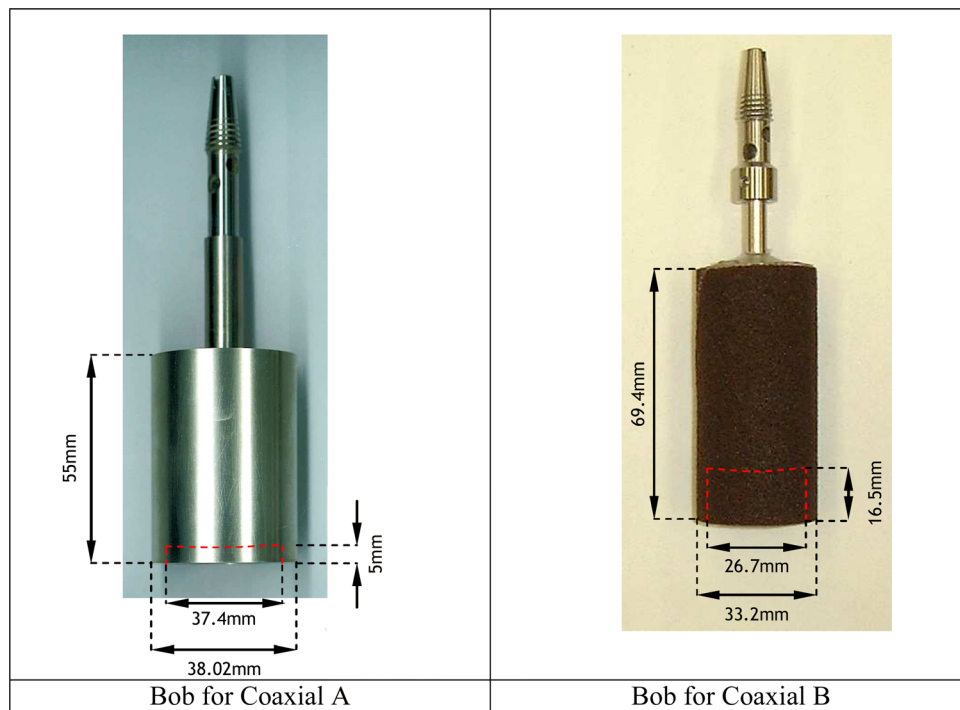


FIG. 8—Coaxial bobs.

Results and Discussion

As stated in the Introduction, a non-Newtonian rheological reference material for cement paste should have five characteristics. Therefore, as the first test, all proposed mixtures were analyzed to determine whether their shear stress–shear rate curves were linear, and the segregation was monitored through visual observation of the material at rest in a closed container.

Test results for the mixture of welan gum and water are shown in Fig. 9. The flow curve measured was not linear over the range of shear rates tested. Also, welan gum requires a biocide to keep the mixture from deteriorating over time. Handling biocide in large quantities, such as that needed

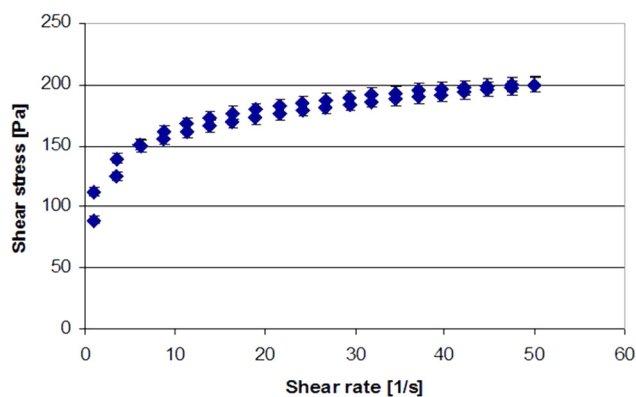


FIG. 9—Curve of shear stress versus shear rate for welan gum in water.

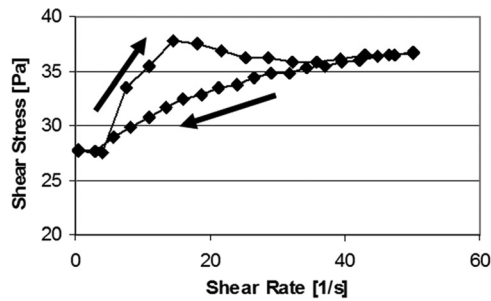


FIG. 10—Flow curve of silica fume–water mixture. There is a large hysteresis, and the down curve is not linear.

for a concrete rheometer, and disposing of it safely are issues that, at this point, are not resolved. Therefore, this candidate is not viable as a reference material for cement paste.

The second mixture examined was SF in water (the SF/water mass ratio was 0.66). A small dosage (0.2% by mass of SF) of polyacrylate-type HRWRA was added to ensure good dispersion. A typical result is shown in Fig. 10. It can be observed that there was a large hysteresis, and also that the down curve was not linear.

A better result was obtained when quartz powder was added to the SF and water mixture according to the following proportions: quartz/SF = 8, water/solid = 0.45 by mass. This yielded a 46% volume concentration of solid particles. Figure 11 shows a typical result obtained. The hysteresis disappeared, but the flow curve still was not linear over the range of tested shear rates. Therefore, this candidate was discarded as well.

The last mixture examined was prepared with corn syrup, water, and limestone powder. As there were three types of limestone and two types of corn syrup, several trials were conducted to determine the optimum composition using these two criteria.

- L-US and CS-US were mixed at several limestone volume concentrations. Another variable was the amount of water used to dilute the corn syrup (CS-US) in order to avoid having the required torque exceed the capacity of the rheometer.
- L-J and CS-J were mixed at several limestone concentrations by volume. This mixture could be measured by the rheometer without the addition of water, because it already contained sufficient water.

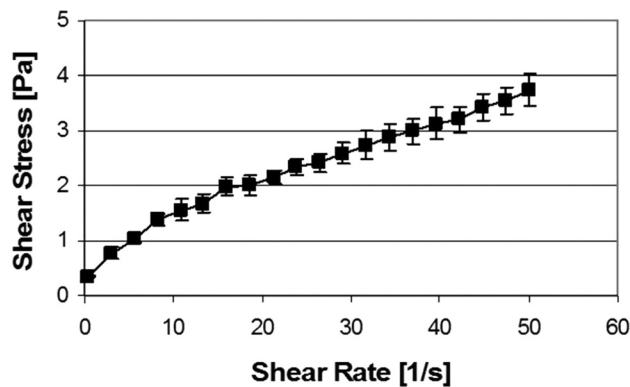


FIG. 11—Flow curve of water–silica fume–quartz mixture, measured with a parallel plate rheometer with a 1 mm gap. The curve is not linear below 20 s^{-1} . The error bars are calculated from three repeat tests (i.e., 1 standard deviation).

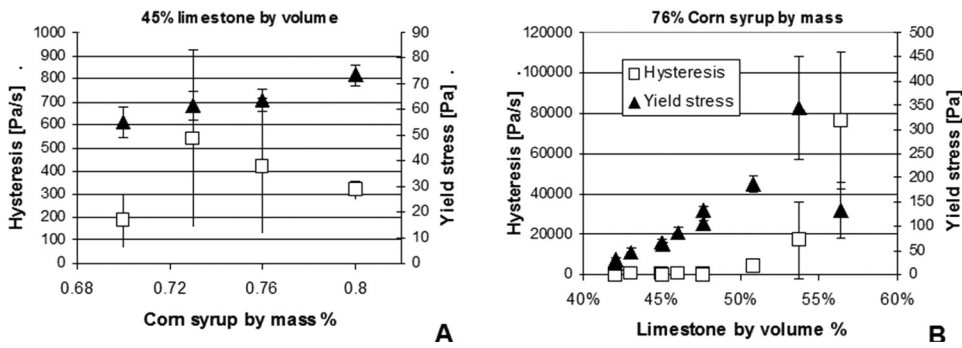


FIG. 12—Comparison of the L-US/CS-US suspension: (a) corn syrup solution in water by mass at constant limestone concentration; (b) limestone volume concentration at constant solution of corn syrup and water. The legend is the same for both graphs. The error bars are calculated from three repeat tests (i.e., 1 standard deviation).

The optimum mixture should have a linear flow curve and high reproducibility, should exhibit an adequate yield stress, and should not exhibit hysteresis in the flow curve. The extent of hysteresis (unit: Pa/s) was defined as the area between the up and down curves of shear stress versus shear rate and is shown in Figs. 12 and 13. Although the down curves of the flow curves of all mixtures were linear, there were significant differences in the hysteresis and yield stress. It could be conceived that the linearity of the down curve should be enough, but for a reference material it was considered preferable to avoid a wide difference between the up and down curves or reduced thixotropy. The hysteresis of the mixtures L-US/CS-US were, with two exceptions, below 700 Pa/s [Fig. 12(a)], whereas the values for the L-J/CS-J mixture were above 1000 Pa/s, and in some cases even as high as 14|700 Pa/s (Fig. 13). It is noted that the particle size distributions of the two types of limestone were very different, which might explain this large discrepancy.

The yield stress was almost zero for most of the L-J/CS-J mixtures, whereas it was above 30 Pa for all L-US/CS-US mixtures. Segregation and random particle interlocking during the measurement are two potential causes of scatter in the experimental results. The particle concentration should be just right, as too low a concentration would increase the risk of segregation, especially when aggregates are added to form mortar or concrete, but too high a particle concentration would lead to flow problems due to particle interlocking. The yield stress necessary in order to avoid

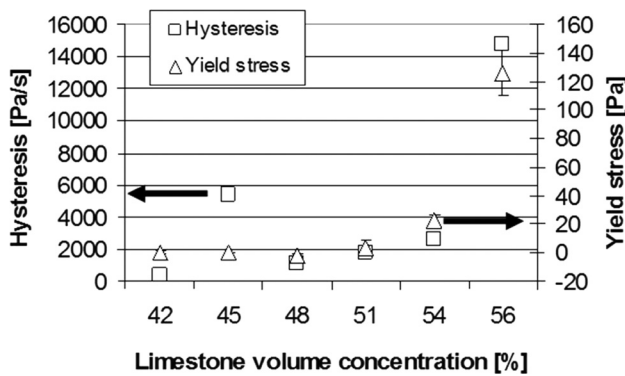


FIG. 13—Comparison of hysteresis and yield stress for all mixtures prepared with L-J and CS-J at various L-J volume concentrations.

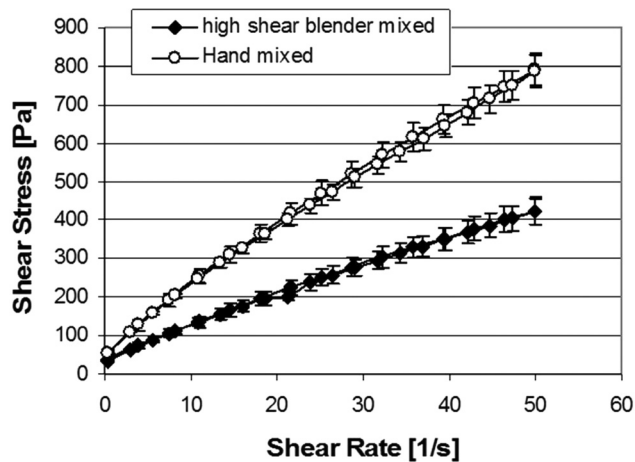


FIG. 14—Flow curves of mixture B mixed by hand and by high shear blender. The error bars are calculated from three repeat tests (i.e., 1 standard deviation).

segregation depends on the density and size of the particles in the mixture. Saak et al. [11] have shown experimentally that a yield stress of over 60 Pa can prevent the sedimentation of aggregates.

It can be stated that the mixture with less than 45 % L-US volume concentration exhibited an adequate yield stress with a low uncertainty and a small hysteresis (Fig. 12). However, the yield stress of the mixture with a greater than 45 % L-US volume concentration had greater uncertainty. Therefore, the best composition of the mixture is a 76 % CS-US aqueous solution and 45 % L-US volume concentration.

The influence of mixing methods was also examined to determine the optimum procedure. Figure 14 and Table 3 show the results obtained with 45 % L-US by volume concentration and 70 % CS-US aqueous solution. Whether the mixture was mixed by hand or with a high-speed blender, the flow curves of the mixture were linear, and there was almost no hysteresis in the two flow curves. This result is very encouraging, as it seems that the linearity and the hysteresis do not depend on the mixing method. However, the values of yield stress and viscosity do depend on the mixing method. In this study, all subsequent mixtures were prepared using the high-speed blender described in the newly approved ASTM C1738 [21].

In the rest of this paper, effects of various factors on the rheological properties are discussed, including pre-mixing duration before the rheological test, mixture degradation versus time at different temperatures, and different types of limestone and corn syrup.

The two mixture proportions used were the following:

- A: L-US 48 % by volume solid concentration, CS-US solution 72 % by mass
- B: L-US 45 % by volume solid concentration, CS-US solution 76 % by mass

TABLE 3—Bingham parameters obtained from Fig. 14.

	Hand Mixing	Mixed by High Shear Blender
Plastic viscosity, Pa · s	14.3 ± 0.8	7.7 ± 0.7
Yield stress, Pa	83.7 ± 1.4	47.5 ± 1.6

Note: All the data are the average of three test results. The uncertainty represents the standard deviation of the three measurements.

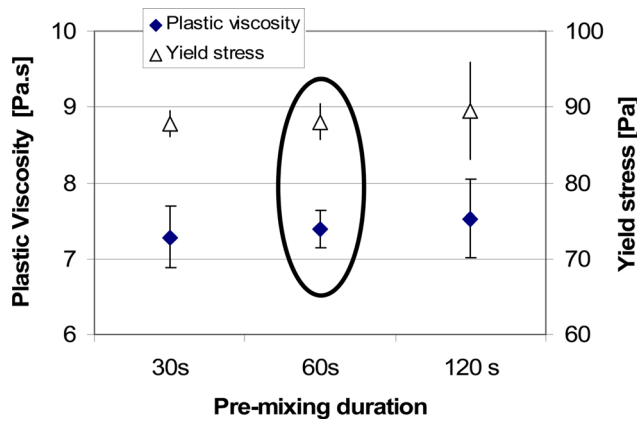


FIG. 15—Influence of pre-mixing. The mixture used was B (L-US + CS-US), with a 2 h rest between the measurements. A 60 s pre-mixing period led to the smallest variability in the yield stress and the least plastic viscosity; R^2 was 0.99 for all the curves. The error bars are calculated from three repeat tests (i.e., 1 standard deviation).

After the initial high shear mixing with the blender, the mixtures needed to be remixed using a homogenizer before the measurements, unless the measurements were done immediately after mixing. Figures 15 and 16 show the test results after re-mixing for different durations using a vane mixer. The tests were conducted directly after mixing with the high-speed blender for 30 s, 60 s, or 120 s. The mixture was left undisturbed for 2 h between mixing cycles to erase any influence of the previous mixing. It was observed that for mixture B, a pre-mixing of 60 s could minimize the measurement uncertainty of the yield stress and plastic viscosity, whereas 120 s was needed for mixture A. All calculations were based only on the down curves.

Next, the type of corn syrup and limestone powder was considered. Figure 17 and Table 4 show the results obtained with the three types of limestone and two types of corn syrup at a 45 % by volume concentration of limestone. The use of CS-J significantly increased the hysteresis relative to the CS-US. The only explanation available at this point is that the type of sugar plays a role, but we have no evidence or reference. CS-US is pure glucose, whereas CS-J is a mixture of glucose and fructose. The combination of L-J and CS-US gives a yield stress that is too low. Therefore, there are two mixtures that could be used as reference materials: L-US + CS-US and L-JFine + CS-US.

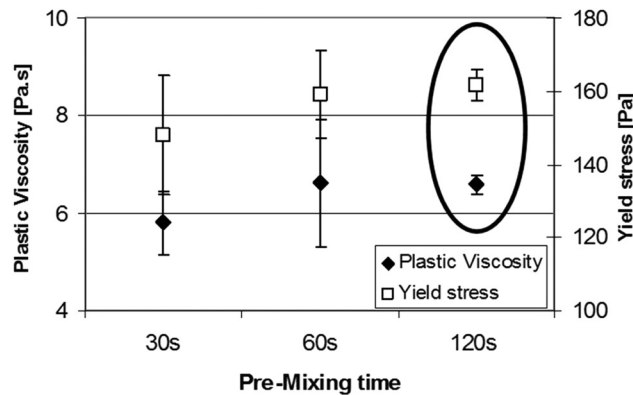


FIG. 16—Influence of pre-mixing after 24 h. The mixture used was A (L-US + CS-US), with a 2 h rest between the measurements. A 120 s pre-mixing period led to the least uncertainty. The error bars are calculated from three repeat tests (i.e., 1 standard deviation).

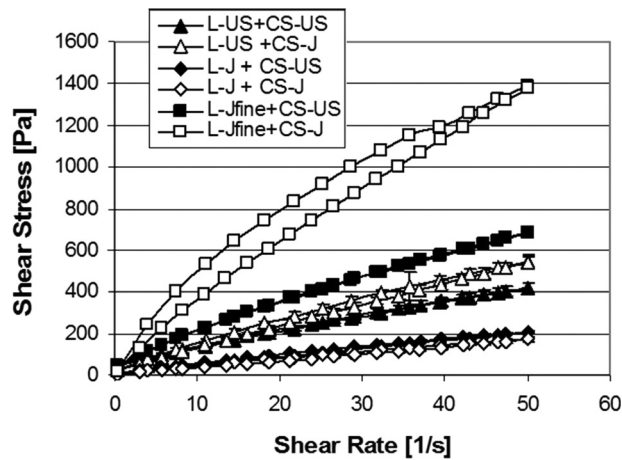


FIG. 17—Flow curves of the various limestone and corn syrup pastes, all at 45% limestone concentration by volume.

Once the mixtures have been selected, it is also important to ensure that there is no deterioration of the material. Both mixtures were examined in regard to deterioration with time and temperature, as well as the repeatability of the rheological measurements. The mixtures were prepared, and half of them were stored at 23°C, while the other half were stored at 6°C. The rheological parameters of the mixtures were then measured after different elapsed times at 23°C. Care was taken for the mixture stored at 6°C to wait for the mixture to reach 23°C before testing it. Figure 18 shows the results obtained. The values of the mixtures did not significantly change for 10 days. The uncertainty for the mixture of L-US + CS-US was below 0.4 Pa · s for the viscosity, independent of the temperature, but the yield stress uncertainty was greater at 23°C (4 Pa to 7 Pa) than at 6°C (3 Pa to 4 Pa). In contrast, the errors obtained for the mixture of L-JFine + CS-US were larger at both temperatures. The yield stress error reached about 10 Pa. These error values are comparable with the values obtained from repeats with fresh mixtures. Therefore, it seems that the combination of L-US + CS-US is best suited for use as a reference material.

TABLE 4—Rheological parameters of the mixtures with the various limestones and corn syrups, all at 45% limestone concentration by volume (see Fig. 17).

Material	Plastic Viscosity, Pa · s	Yield Stress, Pa	Hysteresis Area, Pa/s	Comments
L-US + CS-US	7.4 ± 0.4	62 ± 2	298	Small hysteresis Adequate yield stress
L-US + CS-J	10.4 ± 0.5	27 ± 1	952	Moderate hysteresis Too-small yield stress
L-J + CS-US	3.6 ± 0.1	14 ± 1	324	Too-small yield stress
L-J + CS-J	3.4 ± 0.2	0.3 ± 0.1	5408	High hysteresis Too-small yield stress
L-Jfine + CS-US	21 ± 1	62 ± 5	204	Small hysteresis Adequate yield stress
L-Jfine + CS-J	44 ± 3	62 ± 6	5091	High hysteresis

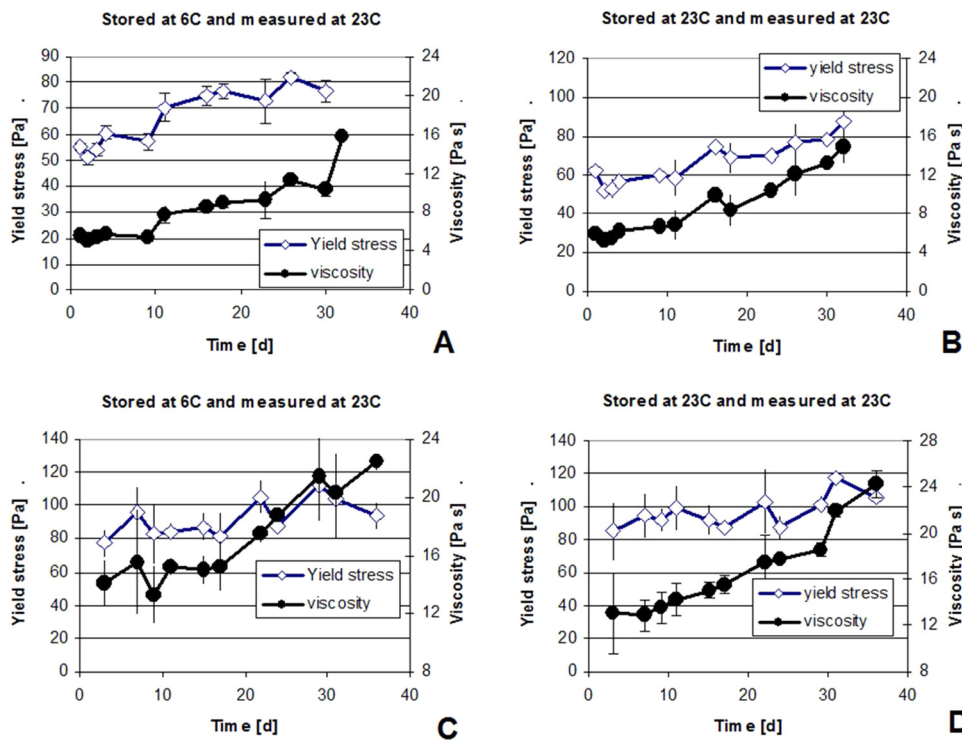


FIG. 18—Evolution of the rheological properties with time: (a),(b) mixture L-US + CS-US (from Table 4); (c),(d) mixture of L-J-fine and CS-US (Table 4).

It is not clear why the rheological properties of yield stress and viscosity increased after 10 days. The following are some potential reasons:

- Slow dissolution of the limestone by the corn syrup solution (the corn syrup solution pH was about 3 to 4). This dissolution would change the composition of the liquid phase and decrease the particle size of the limestone, thus changing the viscosity of the mixture.
- Slow water absorption in the pores of the limestone would effectively increase the particle concentration by decreasing the volume of water between the particles.

Further studies would be needed to determine the true reasons for this behavior.

Table 5 shows a summary of the evaluation of the various materials. It is clear that the only viable reference material would be the mixture of corn syrup with limestone and water, as it fulfills all the requirements.

TABLE 5—Summary of the evaluation of the materials.

Material	1: Segregation	2: Linear Bingham	3: Chemically Stable	4: Yield Stress High	5: Hysteresis
Required answers	NO	YES	YES	YES	NO
Silica fume + quartz + water	NO	NO	YES	N/A	YES
Welan gum + water	NO	NO	YES with biocide	N/A	NO
Corn syrup + limestone + water	NO	YES	YES for 10 days	YES	NO

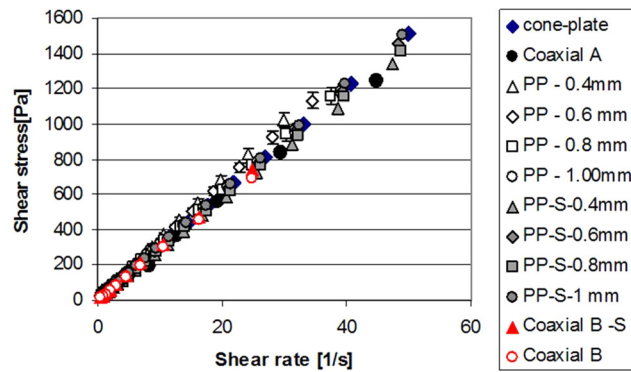


FIG. 19—Measurements using a standard oil with a nominal viscosity of $29.4 \text{ Pa} \cdot \text{s}$. PP, parallel plate with serrated plates; PP-S, parallel plate with a smooth surface. See text for more details.

Tests With Other Rheometer Geometries

Calibration Verification Using Standard Oil

The goal of this work was to develop a reference material that can be used to calibrate rheometers with different geometries. Therefore, we used our optimized mixture in three types of rheometers, as described in the section “Experimental Setup” (i.e., parallel plate, coaxial [two types], and vane).

All the rheometers of various geometries, with the exclusion of the vane, should provide results in fundamental units, as the shear stress and shear rate can be calculated from the torque and rotational speed [22]. Nevertheless, it is essential to verify this assumption by using a standard oil. The oil used was Cannon S8000⁵ (poly(1-butene) 100 %) with a nominal viscosity of $29.4 \text{ Pa} \cdot \text{s}$ at 23°C , as calculated from interpolation between the data provided by the manufacturer. All data obtained using this oil are shown in Fig. 19. Rheometer geometries of parallel plates with smooth and serrated surfaces were used, although only the serrated surface could be used with granular materials to avoid slippage [23]. Also, a rheometer geometry of a cone and plate with a diameter of 25 mm was used with oil for calibration.

The serrated parallel plate (PP in Fig. 19) results measured at different gaps (0.4 mm, 0.6 mm, 0.8 mm, and 1.0 mm) were corrected as outlined by Ferraris et al. [7]. This correction consists of modifying the gap by 0.27 mm to account for the zero error introduced by the plate roughness [24,25]. The smooth parallel plates (PP-S in Fig. 19) also needed a gap correction, but of only 0.022 mm [7] for each of the measured gaps (0.4 mm, 0.6 mm, 0.8 mm, and 1.0 mm) to account for the zero error in the gap.

The coaxial shear stress is calculated from the torque measured using the following formula [26]:

$$\tau = \frac{T}{2\pi LR_b^2} \quad (2)$$

where:

T = torque, $\text{N} \cdot \text{m}$,

L = length of the bob, m, and

R_b = diameter of the bob, m.

⁵Commercial equipment, instruments, and materials mentioned in this paper are identified in order to foster understanding. Such identification does not imply recommendation or endorsement by the National Institute of Standards and Technology (NIST), nor does it imply that the materials or equipment identified are necessarily the best available for the purpose.

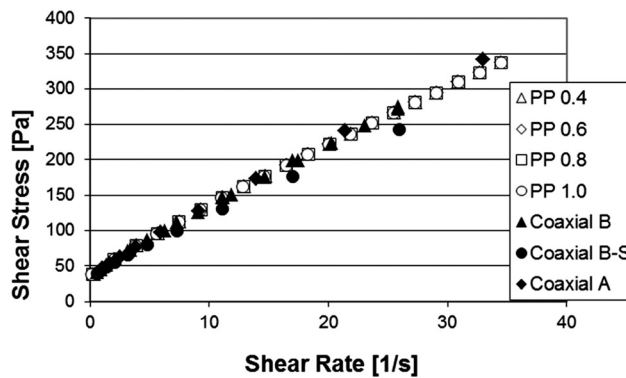


FIG. 20—Rheological measurements of L-US + CS-US (45 % limestone by volume/76 % corn syrup aqueous solution by mass) with a parallel plate (Newtonian approximation) at various gaps and with the two coaxial rheometers. Only the down curves are shown for clarity.

From the results shown in Fig. 19, the average viscosity of the standard oil was determined to be $29.9 \text{ Pa} \cdot \text{s} \pm 1.4 \text{ Pa} \cdot \text{s}$, with a 2 % error relative to the nominal viscosity of the standard oil used ($29.4 \text{ Pa} \cdot \text{s}$). This is an acceptable uncertainty. As all the curves in Fig. 19 are overlapping, we can deduce that there is no slippage [7,23].

Results Using the Proposed Reference Material

All the measurements performed to develop the reference material were done using a serrated parallel plate rheometer at a fixed gap of 0.4 mm. The gap was selected because it is about the average distance between aggregates in a concrete [27]. It should be noted that the material will not stay between the plates if the gap is larger than 1 mm, and a gap smaller than 0.4 mm will result in jamming of the particles [27].

The reference material should provide the same stress-rate curve for all the rheometer geometries providing results in fundamental units. The cone-and-plate setup is the only geometry that cannot be used, as the gap between the truncated cone and the plate is too small to avoid jamming of the limestone particles.

Figure 20 and Table 6 show the results of tests using a new batch of the mixture to ensure that it was fresh and appropriately mixed. Therefore, these data are different from those reported earlier, as the data obtained previously were the results of several attempts to obtain mixtures with Bingham properties. These results were obtained using the developed technique and should reflect the

TABLE 6—Yield stress and plastic viscosity calculated for various rheometer geometries. The parallel plates used the Newtonian approximation.

Geometry	Viscosity, Pa · s	Yield Stress, Pa	Hysteresis, Pa/s
PP 0.4 mm	7.8 ± 0.7	45.5 ± 2.0	12 ± 2
PP 0.6 mm	8.3 ± 1.0	45.7 ± 3.1	48 ± 41
PP 0.8 mm	9.4 ± 0.4	49.5 ± 1.0	48 ± 38
PP 1.0 mm	8.8 ± 1.0	46.7 ± 4.7	18 ± 21
Coaxial A	9.2 ± 0.3	41.9 ± 0.4	22 (one measurement)
Coaxial B, serrated	7.9 ± 0.1	38.3 ± 0.8	34 ± 48
Coaxial B, smooth	9.2 ± 0.1	40.3 ± 0.4	53 ± 5

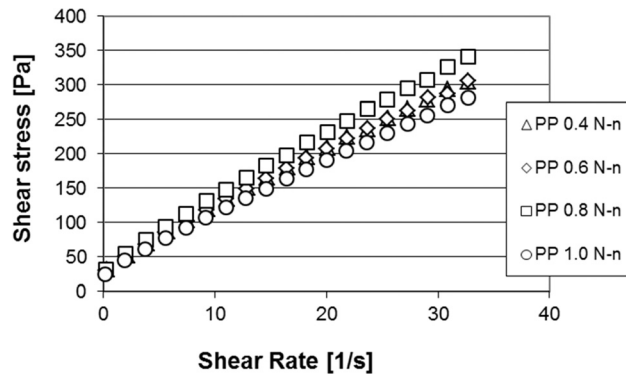


FIG. 21—Rheological measurements of L-US + CS-US (45 % limestone by volume/76 % corn syrup aqueous solution by mass) with a parallel plate at various gaps using the non-Newtonian correction. Only the down curves are shown for clarity.

correct reference material properties. An extensive experimental design has been developed to determine the true uncertainty and repeatability of the results [28]. The first observation is that all curves are within the error (5 % to 10 %, as shown below) of the measurement [28].

The data were processed in the same way as described above while using oil (Fig. 20, and with the non-Newtonian correction for the parallel plate in Fig. 21).

For the parallel plate geometries, a more detailed analysis needs to be performed [29]. The shear rate was calculated as follows for the parallel plates:

$$\dot{\gamma}_R = \frac{R_p}{h} \cdot 2\pi \cdot n \tag{3}$$

where:

- $\dot{\gamma}_R$ = shear rate at the outer edge, 1/s,
- R_p = radius of shear, mm (17.5 mm in our case),
- h = gap or distance between the plates, mm, and
- n = speed of rotation of the top plate, revolutions, 1/s.

The shear stress calculation from the torque is [28]

$$\tau = \frac{T_e}{2 \cdot \pi \cdot R_p^3} \left(3 + \frac{d \ln T_e}{d \ln \dot{\gamma}_R} \right) \tag{4}$$

where:

- τ = shear stress, Pa,
- T_e = torque at the outer edge, N · m,
- R_p = radius of shear, mm (17.5 mm in our case), and
- $\dot{\gamma}_R$ = shear rate at the outer edge, 1/s.

For Newtonian liquids, the factor $d \ln T_e / d \ln \dot{\gamma}_R$ is equal to 1. In our case, with a non-Newtonian material, it was found that it varies with the shear rate (Fig. 21). If the shear rate is above 5 s^{-1} , then the value is 0.8 ± 0.1 , and it decreases to 0.2 for shear rates below 5 s^{-1} . The viscosities were calculated using both methods with an error of less than 3 %, whereas the yield stress error was more significant (up to 20 %) (see Tables 6 and 7 for non-Newtonian results). Table 8 shows the average Bingham parameters for either only parallel plates or all the geometries

TABLE 7—Yield stress and plastic viscosity calculated for various gaps of parallel plates using a non-Newtonian approximation.

Geometry	Viscosity, Pa · s	Yield Stress, Pa
PP 0.4 mm	7.6 ± 0.7	37.0 ± 0.9
PP 0.6 mm	8.1 ± 1.0	37.2 ± 0.6
PP 0.8 mm	9.1 ± 0.4	40.4 ± 0.3
PP 1.0 mm	8.4 ± 1.0	36.3 ± 0.6

considered for both Newtonian and non-Newtonian calculations. Note that the viscosity is within the measurement uncertainty whether the Newtonian or non-Newtonian approximation is used for the calculation for the parallel plates. The greater difference between the two calculations can be seen from the yield stress. Obviously, as the major difference is due to the parallel plate calculation, the uncertainty is reduced overall if a non-Newtonian calculation is used. In the development of a reference material, the calculation method needs to be determined; a non-Newtonian approximation is likely adequate.

In Table 6, the hysteresis area is also shown, and is very low, as expected. The high standard deviation appears because the hysteresis varies from 0 to a value below 100 for the same mixture and geometry.

The scatter between the values (Table 6) obtained with the various geometries is acceptable. To develop the reference value, an extensive statistical study of the variation should be explored [28].

Measurements were performed with a vane rheometer; the data are shown in Fig. 22. The only analytical solution of a vane is for static yield stress [30], and not for a full Bingham equation. Therefore, the slope and intercept, proportional to the yield stress and plastic viscosity, are not expressed in fundamental units and were found to be as follows:

- Yield stress value: $0.6 \pm 0.2 \text{ N} \cdot \text{m}$ (coefficient of variation of 38 %). This large variation is probably due to the very low yield stress measured.
- Viscosity value: $0.354 \pm 0.001 \text{ N} \cdot \text{m} \cdot \text{s}$ (coefficient of variation of 0.2 %).

No fundamental units can be used for the vane rheometer, as the shear rate and shear stress are not known because of the geometry. Correction factors were calculated using the data obtained with known geometries (Table 8) and are as follows:

- Yield stress: 65 (non-Newtonian)
- Viscosity: 24.0 (non-Newtonian)

Modeling of the flow in a vane rheometer is under way at NIST in order to validate this calibration.

TABLE 8—Yield stress and plastic viscosity averages calculated using the Newtonian and non-Newtonian approximations for all geometries.

Geometry	Viscosity, Pa · s		Yield Stress, Pa	
	Newtonian	Non-Newtonian	Newtonian	Non-Newtonian
PP all gaps	8.3 ± 0.6	8.6 ± 0.7	47 ± 2	38 ± 2
PP all gaps and all coaxial	8.7 ± 0.7	8.5 ± 0.7	44 ± 4	39 ± 2

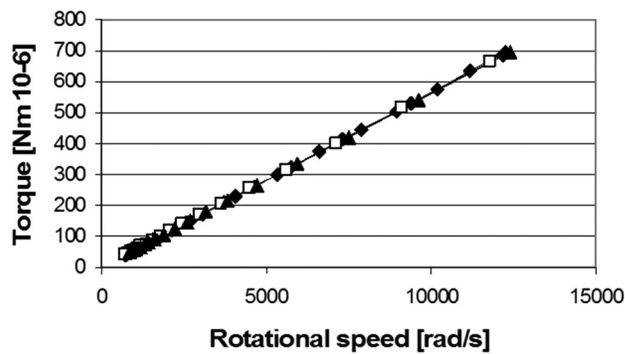


FIG. 22—Rheological measurements of L-US + CS-US (45 % limestone by volume/76 % corn syrup aqueous solution by mass) with a vane geometry. All three measurements are shown.

Conclusions

In this study, a reference material for paste was developed. The materials selected were a mixture of corn syrup, water, and limestone powder. The best composition of the mixture was a 76 % CS-US aqueous solution and 45 % L-US volume concentration. The mixture has the characteristics of a Bingham fluid, is low-cost, and is deterioration resistant for up to 10 days, especially if stored at 6°C while not in use. The Bingham values were approximated here, but a full statistical analysis will be required to have the reference values. The effect of the mixing method on the test results of the Bingham constants was discussed. It was found that appropriate pre-mixing is necessary in order to reduce the experimental error in the shear stress–shear rate curve. However, for producing this kind of reference material, the corn syrup and the characteristics of the limestone powder must be carefully selected. Properties of the limestone that were examined included PSD and surface area as determined by BET theory, and some mineralogy and particle morphology. A more detailed characterization is needed in order for one to fully understand the essential characteristics of a limestone and be able to specify one for selection. Tests such as powder flowability or tribo-electrification [31] could be considered. It was determined that it is essential that the corn syrup be pure glucose rather than a mixture of glucose and fructose.

Using this mixture, many tests should be performed to determine the reproducibility. NIST will pursue this research to develop a standard reference material for cement paste. Then, scale-up to mortar and concrete via the addition of sand and coarse aggregates must be studied. Simulation models would need to be considered to establish the reference rheological properties of mortar and concrete reference materials, as no calibrated rheometer exists for these materials.

Acknowledgments

The writers thank Christina Arnaout, SURF student, for collecting all the data related to the use of silica fume, and Pierre-Jean Bouthors for developing the coaxial B rheometer while doing his Master's thesis at NIST. The contribution of Dr. Brian Lang, NIST, in performing the corn syrup analysis was invaluable. This paper could not have been completed without the help of John Winpigler and Max Peltz, NIST, who performed most of the measurements. The comments received from Dale Bentz, Kenneth Snyder, and Vincent Hackley have significantly improved this paper, and the writers are very grateful.

References

- [1] Hackley, V. A. and Ferraris, C. F., 2001, "The Use of Nomenclature in Dispersion Science and Technology," NIST Recommended Practice Guide SP 960-3, http://www.nist.gov/manuscript-publication-search.cfm?pub_id=850489 (Last accessed 22 March 2013).
- [2] Swindells, J. F., Hardy, R. C., and Cottingham, R. L., "Precise Measurements With Bingham Viscometers and Cannon Master Viscometers," *J. Res. Natl. Inst. Stand. Technol.*, Vol. 52, No. 3, 1954, pp. 105–115.
- [3] ISO/TR 3666, 1998, "Viscosity of Water," *International Organization for Standardization*, Geneva, Switzerland.
- [4] "Comparison of Concrete Rheometers: International Tests at MB (Cleveland OH, USA)," 2003, *NISTIR 7154*, C. F. Ferraris and L. Brower, Eds., <http://concrete.nist.gov/CREMEpapers/Concrete/Calibration/USA-2003-NISTIR-7154.pdf> (Last accessed 22 March 2013).
- [5] Brower, L. and Ferraris, C. F., "Comparison of Concrete Rheometers," *Concr. Int.*, Vol. 25, No. 8, 2003, pp. 41–47.
- [6] "Comparison of Concrete Rheometers: International Tests at LCPC (Nantes, France)," 2000, *NISTIR 6819*, C. F. Ferraris and L. Brower, Eds., <http://concrete.nist.gov/CREMEpapers/Concrete/Calibration/France-2000-NISTIR-6819.pdf> (Last accessed 22 March 2013).
- [7] Ferraris, C. F., Geiker, M., Martys, N. S., and Muzzatti, N., "Parallel-Plate Rheometer Calibration Using Oil and Lattice Boltzmann Simulation," *J. Adv. Concr. Technol.*, Vol. 5, No. 3, 2007, pp. 363–371.
- [8] Spangenberg, J., Roussel, N., Hattel, J. H., Stang, H., Skocek, J., and Geiker, M. R., "Flow Induced Particle Migration in Fresh Concrete: Theoretical Frame, Numerical Simulations and Experimental Results on Model Fluids," *Cem. Concr. Res.*, Vol. 42, No. 4, 2012, pp. 633–641.
- [9] Mikanovic, N., Jolicoeur, C., Khayat, K., and Page, M., "Model Systems for Investigation of the Stability and Rheological Properties of Cement-Based Materials," *ACI Special Publication SP-235*, Vol. 22, American Concrete Institute, Farmington Hills, MI, 2006, pp. 323–356.
- [10] Ferraris, C. F., "Concrete Rheology: Knowledge and Challenges," *2nd International RILEM Symposium on Advances in Concrete through Science and Engineering*, Québec, Canada, RILEM, Bagneux, France, 2006.
- [11] Saak, A. W., Jennings, H. M., and Shah, S. P., "New Methodology for Designing Self-Compacting Concrete," *ACI Mater. J.*, Vol. 98, No. 6, 2001, pp. 429–439.
- [12] Martys, N. S., Ferraris, C. F., Gupta, V., Cheung, J. H., Hagedorn, J. G., Peskin, A. P., and Garboczi, E. J., "Computational Model Predictions of Suspension Rheology: Comparison to Experiment," *12th International Congress of the Chemistry of Cement*, Montréal, Canada, July 8–13, 2007, National Research Council of Canada Institute for Research, Ottawa, Ontario, Canada.
- [13] Sakai, E., Hoshimo, S., Ohba, Y., and Daimon, M., "The Fluidity of Cement Paste With Various Types of Inorganic Powders," *Proceedings of the 10th International Congress on the Chemistry of Cement*, Gothenburg, Sweden, June 2–6, 1997.
- [14] Ferraris, C., Obla, K., and Hill, R., "The Influence of Mineral Admixtures on the Rheology of Cement Paste and Concrete," *Cem. Concr. Res.*, Vols. 31–32, 2001, pp. 245–255.
- [15] Hwang, H.-J., Lee, S.-H., and Sakai, E., "Rheological Behavior of Slag Cement Paste Prepared by Adjusting the Particle Size Distribution," *J. Ceram. Proc. Res.*, Vol. 10, No. 4, 2009, pp. 409–413.

- [16] Aral, B. K. and Kalyon, D. M., "Effects of Temperature and Surface Roughness on Time Dependent Development of Wall Slip in Steady Torsional Flow of Concentrated Suspensions," *J. Rheol.*, Vol. 38, No. 4, 1994, pp. 957–972.
- [17] Nickerson, C. S. and Kornfield, J. A., "A Cleat Geometry for Suppressing Wall Slip," *J. Rheol.*, Vol. 49, No. 4, 2005, pp. 865–874.
- [18] Kalyon, D. M., "Apparent Slip and Viscoplasticity of Concentrated Suspensions," *J. Rheol.*, Vol. 49, No. 3, 2005, pp. 621–640.
- [19] Helmuth, R., Hill, L., Whitting, D., and Bhattacharja, S., "Abnormal Concrete Performance in the Presence of Admixtures," *PCA R&D Report No. 2006*, Portland Cement Association, Skokie IL, 1995.
- [20] Bouthors, P.-J., 2008, "Concrete Rheology: Calibration of IBB Rheometer With a Suspension of Bentonite," M.S. thesis Univ. de Bretagne Sud, Lorient France.
- [21] ASTM C1738: "Standard Practice for High-Shear Mixing of Hydraulic Cement Pastes," *Annual Book of ASTM Standards*, ASTM International, West Conshohocken, PA.
- [22] Coussot, P., Tocquer, L., Lanos, C., and Ovarlez, G., "Macroscopic vs. Local Rheology of Yield Stress Fluids," *J. Non-Newtonian Fluid Mech.*, Vol. 158, 2009, pp. 85–90.
- [23] Buscall, R., McGowan, J. I., and Morton-Jones, A. J., "The Rheology of Concentrated Dispersions of Weakly Attracting Colloidal Particles With and Without Wall Slip," *J. Rheol.*, Vol. 37, No. 4, 1993, pp. 621–641.
- [24] Davies, G. A. and Stokes, J. R., "On the Gap Error in Parallel Plate Rheometry that Arises from the Presence of Air When Zeroing the Gap," *J. Rheol.*, Vol. 49, No. 4, 2005, pp. 919–922.
- [25] Sanchez-Perez, J. and Archer, L. A., "Interfacial Slip Violations in Polymer Solutions: Role of Microscale Surface Roughness," *Langmuir*, Vol. 19, 2003, pp. 3304–3312.
- [26] Schramm, G., *A Practical Approach to Rheology and Rheometry*, Gebrueder Haake GmbH, Karlsruhe, Germany, 1994, <http://www.polymer.cn/bbs/File/UserFiles/Upload/200904010309415s.pdf> (Last accessed 22 March 2013).
- [27] Garboczi, E. J. and Bentz, D. P., "Analytical Formulas for Interfacial Transition Zone Properties," *Adv. Cem. Based Mater.*, Vol. 6, 1997, pp. 99–108.
- [28] Ferraris, C. F., Stutzman, P., Guthrie W., and Winpighler, J., 2012, "Certification of SRM 2492: Bingham Paste Mixture for Rheological Measurements," NIST SP 260-174, http://www.nist.gov/manuscript-publication-search.cfm?pub_id=911268 (Last accessed 1 March 2013).
- [29] Collyer, A. A. and Clegg, D. W., *Rheological Measurements*, Chapman & Hall, London, 1998.
- [30] Dzuy, N. Q. and Boger, D. V., "Yield Stress Measurement for Concentrated Suspensions," *J. Rheol.*, Vol. 27, No. 4, 1983, pp. 321–349.
- [31] Diederich, P., Mouret, M., de Ryck, A., and Pochon, F., "Dry State Properties of Limestone Fillers in Relation to Their Flow Properties in Suspension for an Understanding of SCC," *3rd RILEM Symposium on Rheology of Cement Suspensions Such as Fresh Concrete*, Reykjavik, Iceland, August 19–21, 2009, RILEM, Bagneux, France, pp. 245–253.